Renewable Energy 120 (2018) 457–467

Contents lists available at ScienceDirect

Renewable Energy

journal homepage: www.elsevier.com/locate/renene

Surface turbulence intensity as a predictor of extrapolated wind resource to the turbine hub height: method's test at a mountain site

Giovanni Gualtieri

National Research Council, Institute of Biometeorology (CNR-IBIMET), Via Caproni 8, 50145, Firenze, Italy

ARTICLE INFO

Article history:
Received 27 May 2017
Received in revised form
14 November 2017
Accepted 1 January 2018
Available online 3 January 2018

Keywords:
Wind resource extrapolating methods
Turbulence intensity
Wind shear coefficient
Atmospheric stability
Mountain site
Wind energy yield

ABSTRACT

Following testing at the Cabauw (Netherlands) flat and inland site, and at the FINO3 offshore platform in the North Sea (Germany), the α–I wind resource extrapolating method was tested at the Boulder (CO, USA) mountain site (1855 m), another substantially different location in terms of surface characteristics, stability conditions, and wind energy pattern. Data from local 82-m M2 met mast between 10 and 80 m were used, with extrapolations to 50-m and 80-m turbine hub heights performed based on 10-m and 20-m turbulence intensity observations. Trained over a 2-year period (1997–1998), the method was validated on the year 1999.

Slightly better results than those at both Cabauw and FINO3 were achieved in 50-m and 80-m wind speed extrapolations, with bias within 5%, NRMSE = 0.17–0.23, and $r = 0.96$–0.98. In predicting the annual energy yield, a bias within 1% was achieved at 50 m, which at worst increased to 6.44% at 80 m. The method was less stability-sensitive than at Cabauw and particularly FINO3. It proved to be reliable even over a mountain site affected by fairly complex terrain, which is noteworthy if considering the power law the method is based upon was actually developed for flat and homogeneous terrain.

1. Introduction

Wind data are generally measured significantly below the WT hub height, thus requiring lower wind measurements to be adjusted to the WT hub height by using a reliable wind speed extrapolation model [1]. Modern multi-MW WTs operate at heights well above the surface layer, thus becoming necessary that such an extrapolation model be valid up to at least 150–200 m [2]. In wind energy studies, PL and LogL are the most widely used wind speed extrapolation models [3]. Although LogL is quite accurate near the surface, its accuracy proved to decrease as the height grows [4], which becomes an issue when dealing with modern multi-MW WTs. Since further from the surface evidences suggested that the wind speed vertical profile has a PL form [4], the use of PL is generally preferred. However, careful estimation of the PL exponent α (or WSC) is crucial for applying this model, as a rough α assessment may result in inaccurate energy yield predictions (e.g. Refs. [5,6]). With this in mind, a method making use of surface turbulence intensity I as a predictor of α, and thus of extrapolated wind resource to the WT hub height via application of the PL, has been recently proposed [7,8]. Originally developed and validated at Cabauw (Netherlands), a flat and sea-level inland site, based on data collected between 10 and 80 m from the KNMI 213-m tall met mast [7], this α–I method was then tested at the FINO3 offshore platform in the North Sea (Germany) based on records collected between 30 and 100 m from the BSH 120-m tall met tower [8]. The goal of this work is thus to provide further insight into its application field by testing the method over an elevated mountain site, significantly different from the other two in terms of surface characteristics, stability conditions, and wind energy pattern.

Winds associated with mountainous terrain are generally of two types: (i) terrain-forced flows, produced when large-scale winds are modified or channelled by the underlying complex terrain; (ii) thermally-driven circulations, produced by temperature contrasts that form within the mountains or between the mountains and the surrounding plains [9]. Wind speed is generally increased on hill and mountain locations: this results from altitude, as hill tops and mountain peaks extend high into the atmosphere where wind speeds are higher, as well as from wind flow acceleration over and around hills and mountains, and funnelling through passes or along valleys aligned with the flow [10]. However, valleys, basins, and lee slopes within a mountain area are often sheltered from the generally stronger winds at high altitudes by the surrounding

E-mail address: g.gualtieri@ibimet.cnr.it.

https://doi.org/10.1016/j.renene.2018.01.001
0960-1481/

Nomenclature

Abbreviations

AGL	above ground level
ASL	above sea level
BSH	Bundesamt fuer Seeschifffahrt und Hydrographie
KNMI	Royal Netherlands Meteorological Institute
LogL	logarithmic law
NWTC	National Wind Technology Center
PL	power law
WSC	wind shear coefficient
WT	wind turbine

Variables

α	wind shear exponent [−]
AEY	annual energy yield [MWh/y]: WT net energy production over a 1-year period
AF	availability factor [%]: time percentage a WT operates between its cut-in and cut-off wind speeds
c	Weibull scale factor [m/s]
CF	capacity factor [%]: ratio of *AEY* to the energy that the WT could have produced if operated at its rated power through the same period
FLH	full-load hours [h/y]: number of hours in one year corresponding to *CF*
I	turbulence intensity [%]
k	Weibull shape factor [−]
P	wind power density [W/m^2]
P_a	pressure [mbar]
ρ	air density [kg/m^3]
σ_θ	standard deviation of wind direction [deg]
σ_u	standard deviation of longitudinal wind speed fluctuation [m/s]
T	temperature [°C]
v	wind speed [m/s]
z	height AGL [m]
z_o	roughness length [m]

Statistical skill scores

IA	index of agreement = $1-[N\cdot RMSE^2/\sum_{i=1}^{N}(\lvert P_i-\overline{O_i}\rvert+\lvert O_i-\overline{O_i}\rvert)^2]$
$\mu_O=\overline{O_i}$	mean observations $=\frac{1}{N}\sum_{i=1}^{N}O_i$
$\mu_P=\overline{P_i}$	mean predictions $=\frac{1}{N}\sum_{i=1}^{N}P_i$
N	number of observations
NB	normalized bias $=\frac{1}{N}\sum_{i=1}^{N}(O_i-P_i)/\sqrt{\overline{O_i}\cdot\overline{P_i}}$
NE	normalized error $=(O_i-P_i)/O_i$
NRMSE	normalized root mean square error $= RMSE/\sqrt{\overline{O_i}\cdot\overline{P_i}}$
O_i	observations
P_i	predictions
r	correlation coefficient $=\frac{1}{N}\sum_{i=1}^{N}(O_i-\overline{O_i})\cdot(P_i-\overline{P_i})/\sigma_O\cdot\sigma_P$
RMSE	root mean square error $=\sqrt{\frac{1}{N}\sum_{i=1}^{N}(O_i-P_i)^2}$
σ_O	standard deviation of observations $=\sqrt{\frac{1}{N-1}\sum_{i=1}^{N}(O_i-\overline{O_i})^2}$
σ_P	standard deviation of predictions $=\sqrt{\frac{1}{N-1}\sum_{i=1}^{N}(P_i-\overline{P_i})^2}$

topography [9]. Also thermal effects may be caused by differences in altitude: cold air from high mountains can sink down to the plains below, causing quite strong and highly stratified downslope winds [10].

Mountainous locations generally exhibit a complex terrain, i.e. great variety of features such as hills, ridges, high passes, plateaus, large escarpments, valleys, and canyons. Since elevations and depressions occur in a random fashion, flow conditions over these features are the most complex to be addressed [11]. As shown within several works (e.g. Refs. [12–16]), numerical meteorological models are unable to resolve the considerable wind speed variability over short distances caused by local terrain features [3], resulting in a certain (up to 13.2% [14]) or even substantial (50% [12], or up to 83.3% [15]) average wind speed over-estimation. Accordingly, the available wind resource over such complex areas depicted by wind maps or atlases is affected by the highest uncertainty degree [13]. Actually, both PL and LogL were developed for flat and homogeneous terrain [3,11], so that any surface irregularities will modify the wind flow through velocity deficits, unusual wind shear, and wind acceleration. This raises serious concerns on applicability of these vertical laws over areas subject to important terrain effects [11], thus making a particularly challenging issue to apply the α–*I* extrapolating method – which is actually a modified PL – over a mountain site affected by a complex terrain. To this goal, observations from an 82-m tall met tower located at the NWTC elevated site near Boulder (CO, USA) were used, including 10-min records collected between 10 and 80 m. Two WT hub heights, 50 and 80 m, were considered for wind resource extrapolation. A linear regression analysis by stability condition through a 2-year period (1997–1998) was performed to train the method, which was later validated over an independent 1-year period (1999) and its accuracy assessed in extrapolating annual mean wind speed, Weibull distribution, and wind energy yield.

With respect to current Boulder application, two general comparisons have been performed throughout the paper: (i) scores of the α–*I* method's application achieved over the other two locations of Cabauw and FINO3 (Table 1); (ii) wind characteristics observed at other elevated sites worldwide, and wind resource extrapolating scores achieved at some of those sites (Table 2).

2. Background

From the PL equation, the exponent α_{12} between heights z_1 and z_2 can be determined once concurrent wind speeds v_1 and v_2 at corresponding heights are available [5]:

$$\alpha_{12} = \frac{\ln(v_2/v_1)}{\ln(z_2/z_1)} \quad (1)$$

Wind turbulence intensity *I* is defined as the ratio between wind speed standard deviation (σ_u) and wind speed average ($\overline{v}$) [11]:

$$I = \frac{\sigma_u}{\overline{v}} \quad (2)$$

with both σ_u and $\overline{v}$ calculated – by convention in wind energy engineering – over 10-min bins.

The existence of a possible relationship between *I* and α was suggested in the past literature [33,34], although with some restrictions applying, including: (i) wind speeds above 10 m/s [34]; (ii) flat and quite smooth terrain ($z_0 \leq 10$ cm) [33]; (iii) near-neutral stability conditions [33,34]; (iv) height of 15 m [34] or 30 m [33].

Within two previous studies [7,8], the exponent α_{12} between z_1

Table 1
Met mast supplied application sites of the α–I method and height bins considered for wind resource extrapolation.

Location (State, Country)	Operator	Altitude (m ASL)	Terrain, and land use	Measurement period (Full years)		Extrap. height bins (m AGL)	Ref.
				Method's training	Method's testing		
Boulder (CO, USA)	NWTC	1855	Fairly complex, hills with no trees	1997–1998	1999	10–50 10–80 20–80	This work
Cabauw (Netherlands)	KNMI	−0.7	Flat, open pasture, 50 km from the coast	2012	2013	10–40 10–80 20–80	[7]
FINO3 (Germany)	BSH	0	Offshore, 80 km off the coast	2011–2012	2013	30–80 30–100	[8]

and z_2 was demonstrated being linearly related to the surface turbulence intensity I_1 at height z_1:

$$\alpha_{12} = bI_1 \tag{3}$$

In addition, restrictions applying in Refs. [33,34] were largely overcome, as validity of Eq. (3) was extended to a wider range of wind speeds ($v \geq 3$ m/s [7], and $v > 0$ m/s [8]), tested over two substantially different (onshore/offshore) environments (Table 1), and generalised to all stability conditions. A linear regression analysis by stability conditions was applied to Eq. (3) to derive the stability-dependent regression coefficients b. A detailed description of this method's development may be found in Ref. [7].

3. Study area and data

The NWTC (http://www.nrel.gov/nwtc) is the US premier wind energy technology research facility. Managed by the National Renewable Energy Laboratory (NREL) for the US Department of Energy, the NWTC is located at the foot of the Rocky Mountains, about 8 km S of Boulder, 11 km W of Broomfield, and 36 km NW of Denver, CO [35]. In the NWTC's 305-acre site small and large WTs for research and development purposes, a photovoltaic array, and various met towers including the two recent 135-m tall M4 and M5 masts (operated since 2012) are installed (Fig. 1) [36].

A long-term wind time series is available from the M2 met mast, which is an instrumented 82-m tall tower located at the western edge of the NWTC site. The tower is located at 39° 54′ 38.34” N and 105° 14′ 5.28” W, at an elevation of 1855 m ASL. M2 data span from Sep. 1996 to the present day and are online at: http://www.nrel.gov/midc/nwtc_m2, where further information and documentation are also available. Air temperatures are measured with platinum resistance thermometers (Met One T200A) at 2, 50, and 80 m, while air pressure is measured at 2.5 m [37].

In the present work, 3 years (01/01/1997 to 31/12/1999) of 10-min M2 mast readings have been used, including average wind speed and direction, standard deviation of wind speed and direction, air temperature, and pressure, obtained (or adjusted) at heights of 10, 20, 50, and 80 m AGL.

The Boulder (NWTC) site is located on a mountain area (mean elevation of 1850 m), characterised by hills with no trees and overall featuring a fairly complex terrain [27]. Site's mean z_0 is reported as 0.14 [28] or 0.15 m [27]. In Fig. 2 the situation on Dec. 2002 is captured, i.e. the one closer to the selected time period. The M2 mast is located in the complex terrain downwind of Colorado's Front Range mountains, with the nearest peak of 2530 m about 4 km away (Fig. 2a). Toward all directions other than W the M2 mast is substantially free from major topographical structures, although small rolling hills and small water bodies may be found in the surroundings (Fig. 2b). Local winds are dominated by WNW flows funneled through the Eldorado Canyon, a prominent canyon about 5 km upwind on an approximate bearing of 292° (Fig. 2a). These stronger WNW winds are more frequent in winter and began in the evenings as the surface cooled and the atmosphere stratified. W weaker winds were also identified being likely due to katabatic flows down the slope of the Front Range or drainage flows [38]. A flow from S more frequent during the spring and summer months, and a northern flow that dominates in the summer, both driven by local thermally-driven circulations, are also effective in the area [36].

4. Data analysis

4.1. Overall meteorological statistics

Table 3 reports the overall annual statistics of main meteorological variables measured between 10 and 80 m during the analysis period (1997–1998). Values of temperature at 10 and 20 m were obtained through a linear interpolation between records at 2 and 50 m. Values of pressure at 10, 20, 50 and 80 m were approximated as a function of temperature at the same heights, pressure at 2.5 m, and height by using the formulation reported, e.g., in Ref. [39]. Thus, according to [40], air density values at the selected heights were calculated based on values of pressure and temperature.

Mean wind speeds observed at M2 mast range between 3.61 and 4.67 m/s. These values agree with those measured within several other studies carried out at the same mast: as reported in Table 2, based on 7 years (1997–2003) of 1-h data, Lubitz [5] reported mean values of 4.62 and 4.81 m/s at 50 and 80 m, respectively; approximately the same dataset was used by Elkinton et al. [27] to derive a mean wind speed value of 4.75 m/s at 50 m; based on a 1-year dataset, Lackner et al. [28] measured wind speed values of 4.60 m/s (50 m) and 4.80 m/s (80 m).

As well as wind speed, air density is quite low (0.993–1.003 kg/m^3), thus also resulting in low power density values (85.5–185.2 W/m^2). Therefore, according to the NREL wind power classification (http://www.nrel.gov/gis/wind_detail.html), Boulder can be classified as a poor (or “class 1”) site, as at 50 m wind speed is below 5.6 m/s and power density below 200 W/m^2.

4.2. Atmospheric stability, WSC and turbulence intensity

Atmospheric stability based on Pasquill stability classes has been calculated by applying the σ_θ method [41] with $z_0 = 0.15$ m (Table 4): neutral conditions (class D) are the most frequent (49.25%), while unstable and stable conditions occur by 28.38 and 22.37%, respectively. If considering the overall values, mean turbulence intensity decreases with height (24.00–20.50%), while mean WSCs range between 0.104 and 0.114 (Table 4). At the same

Table 2
High altitude sites considered for comparison and wind characteristics overall mean values.[a]

Location (State, Country)	Altitude (m ASL)	Measurement period	Height & ht. bin (m AGL)	v (m/s)	k	α	Ref.
Stone Mt (TN, USA)	1300	04/2001–03/2002	50	7.40	2.60		[17]
			30–50			0.280	
Niğde (Turkey)	1300	01/2000–12/2006	10	8.00	1.74		[18]
Duga Poljane (Serbia)	1310	02/2010–01/2011	10–60			0.190	[19]
Boone (NC, USA)	1347	01/1979–12/1979	45.7	7.00	1.78		[20]
			76.2	7.80	1.79		
			18.2–45.7			0.486	
			18.2–76.2			0.378	
Howard's Knob (NC, USA)	1350	01/1977–12/1980	46	7.20	2.10		[17]
			18–46			0.240	
Luning 7W (NV, USA)	1354	08/2003–12/2007	50	3.96	1.34		[21]
			10–50			0.105	
Tucumcari (NM, USA)	1354	11/1980–08/1982	45.7	8.60	2.63		[22]
			9.1–45.7			0.191	
Monte Settepani (Italy)	1375	01/2004–06/2008	10	5.45	1.84		[23]
Livingston (MT, USA)	1420	09/1980–09/1982	45.7	8.40	1.73		[22]
			9.1–45.7			0.132	
Mérida (Venezuela)	1479	01/2005–12/2009	10	2.47			[24]
Luning 5N (NV, USA)	1523	08/2003–12/2007	50	3.81	1.33		[21]
			10–50			0.110	
Tonopah 24NW (NV, USA)	1535	08/2003–12/2007	50	5.49	1.70		[21]
			10–50			0.081	
Clayton (NM, USA)	1536	01/1979–12/1979	45.7	7.30	2.24		[20]
			9.1–45.7			0.202	
Rafsanjan (Iran)	1550	2 years	40	5.41	1.96		[25]
Masitise (Lesotho)	1700	01/2001–12/2002	10	4.93	1.63		[26]
			10–25			0.060	
Bardsir (Iran)	1763	2 years	40	3.27	1.21		[25]
Kars (Turkey)	1768	01/2000–12/2006	10	6.90	1.77		[18]
Kingston 14SW (NV, USA)	1780	08/2003–12/2007	50	4.53	1.41		[21]
			10–50			0.125	
Poggio Fearza (Italy)	1833	01/2007–12/2007	10	4.72	1.51		[23]
Boulder (CO, USA)	1855	01/1997–12/2003	50	4.62			[5]
			80	4.81			
			10–20			0.110	
		09/1996–12/2003	50	4.75			[27]
			10–50			0.100	
		1 year	50	4.60			[28]
			80	4.80			
			20–50			0.190	
Shahrbabak (Iran)	1856	2 years	40	4.29	1.60		[25]
San Augustin Pass (NM, USA)	1859	11/1980–09/1982	45.7	9.30	2.00		[22]
			9.1–45.7			0.152	
Ft. Davis (TX, USA)	1860	07/1998–06/1999	25–40			0.110	[29]
Erzurum (Turkey)	1950	01/2000–12/2006	10	8.70	1.73		[18]
Manisa (Turkey)	2020	01/2000–12/2006	10	7.40	1.71		[18]
UAA-UAZ (Mexico)	2230	08/2005–07/2006	40	4.73			[30]
			20–40			0.159	
Wells (NV, USA)	2268	10/1980–01/1982	45.7	7.80	1.92		[22]
			9.1–45.7			0.084	
Bridger Butte (WY, USA)	2290	09/1980–09/1982	45.7	8.40	1.92		[22]
			9.1–45.7			0.115	
Perote (Mexico)	2398	01/2001–12/2006	40	5.32			[31]
			20–40			0.120	
Albuquerque (NM, USA)	2578	01/2002–12/2002	40	6.80			[32]
			25–40			0.240	

[a] Overall mean values of k and α from Refs. [20,22] are calculated based on Weibull fit to the reported wind speed frequency distribution, and wind sector averaged α values, respectively.

M2 mast (Table 2), Elkinton et al. [27] reported for α_{10-50} a comparable overall value of 0.100, while Lubitz [5] measured $\alpha_{10-20} = 0.110$, and Lackner et al. [28] measured $\alpha_{20-50} = 0.190$.

As shown in Table 2, it is also useful to compare Boulder wind characteristics to those achieved at other high altitude locations worldwide.

Focussing on Boulder similarly elevated sites and taking its α_{10-50} value (0.114) for comparison, a higher value ($\alpha_{9.1-45.7} = 0.152$) was measured on the steep and barren site of San Augustin Pass (1859 m) [22], while closer values were observed elsewhere: α_{10-50} of 0.125 at Kingston 14SW (1780 m) [21], and α_{25-40} of 0.110 at Ft. Davis (1860 m) [29]; conversely, a lower value ($\alpha_{10-25} = 0.060$) was measured at the low grass site of Masitise (1700 m) [26].

At Boulder more elevated sites, a similarly wide range was observed for α: a higher overall α value ($\alpha_{20-40} = 0.159$) was measured at the rural and farming site of UAA-UAZ (2230 m) [30], and even higher ($\alpha_{25-40} = 0.240$) at the far higher location with complex terrain of Albuquerque (2578 m) [32]; comparable values were observed with $\alpha_{20-40} = 0.120$ at Perote (2398 m) [31], and with $\alpha_{9.1-45.7} = 0.115$ at the flat and barren mesa site of Bridger Butte (2290 m) [22]; a lower value ($\alpha_{9.1-45.7} = 0.084$) was measured at the slightly rolling ridge site of Wells (2268 m) [22].

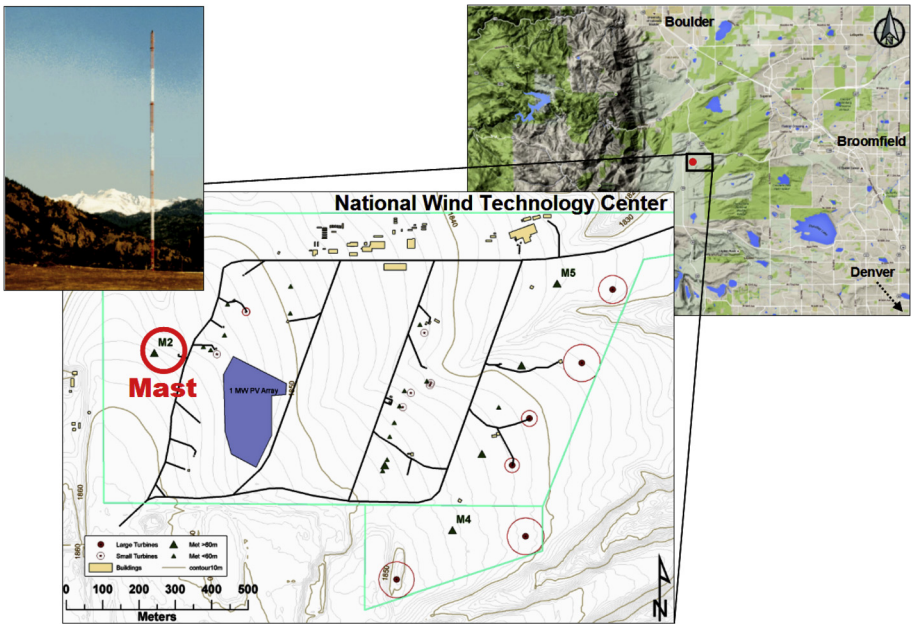

Fig. 1. Map and location of the Boulder (NWTC) site and M2 met mast, also displaying an M2 mast picture (Sources: http://www.nrel.gov/midc/nwtc_m2 and GoogleMaps).

The observed α range was significantly large also if considering locations at a lower altitude than Boulder. Within a survey on ridge mountain sites in Southern Appalachian Mountain region (US), Raichle and Carson [17] reported $\alpha_{30-50} = 0.280$ on Stone Mt (1300 m ASL), and $\alpha_{18-46} = 0.240$ on Howard's Knob (1350 m). With respect to Boulder, the overall α values measured at the 12-m tall trees forested ridgetop site of Boone (1347 m) was remarkably higher: here the relevant site's roughness was the likely cause of such high overall values of $\alpha_{18.2-45.7}$ (0.486) and $\alpha_{18.2-76.2}$ (0.378) [20]. From this survey it is thus confirmed that, besides altitude (and thus large-scale wind speed), α depends on local conditions such as topography, surface roughness and atmospheric stability [33].

At Boulder, the stability-varying WSC pattern is quite uncertain (Table 4): from very stable to very unstable conditions, two relative minima may be observed for WSCs, one for class E, and one for classes B and C. This WSC pattern deviates from the one reported within most of similar surveys in the literature (e.g. Ref. [3]), where observed WSCs steadily increase from unstable to stable conditions. However, similarities – at least for the minimum occurring for classes B and C – have been found in the stability-varying WSC patterns reported by Touma [42], markedly between 10 and 60 m from the rolling site of Missouri ($z_0 = 20$ cm) in the period 1973–1975. Note that at Boulder measured WSCs for class D (0.099–0.125) are quite lower than the $1/7 = 0.143$ default value commonly assumed when no WSC measurements are available at a site. As expected, observed turbulence intensity decreases from unstable to stable conditions, yet with a not monotonic pattern, as a minimum is reached for class E, to then increase for class F. This stability-varying turbulence intensity pattern definitely agrees with the one observed at Cabauw between 10 and 80 m [7].

WSC and turbulence intensity clear dependence on atmospheric stability is apparent in Fig. 3, where their daily and yearly mean courses are plotted vs. the frequency of stability classes.

As well-known (e.g. Refs. [3,6,19]), the WSC daily course (Fig. 3a) is a strict function of the diurnal heating/cooling cycle of air above the ground. At Boulder, hourly WSCs range from 0.058–0.066 at noon to 0.135–0.147 in the night-time, overall exhibiting a 120–140% difference between the extremes. At the site of Ft. Davis (1860 m, Table 2), daily α_{25-40} was observed to vary from 0.050 at noon and early afternoon to 0.175 in the early morning [29].

Turbulence intensity daily course is more time-independent than WSC, showing a 36–38% overall excursion: I_{10} values range 21.00–28.50%, while I_{20} values range 19.70–27.10%. This turbulence intensity daily variation appears anti-correlated to the corresponding WSC variation, with minima in the nocturnal (more stable) hours and maxima in the diurnal (more unstable) hours.

At Boulder, atmospheric stability intra-annual variability (Fig. 3b) is less pronounced than the intra-daily variability, particularly for stable conditions, which occur by 18–26%: unstable conditions occur 16–18% (coldest months) to 38–41% (warmest months), while conversely stable and neutral conditions occur on aggregate 59–62% (warmest months) to 82–84% (coldest months). This smoother stability intra-annual course strongly impacts on both WSC and turbulence intensity, as their courses are smoother as well.

WSC intra-annual variability, showing a global excursion of 45–100%, does not exhibit a regular pattern: for 10–50 and 10–80 m height intervals monthly WSC maxima are observed in June and July (0.124–0.137), i.e. when stable conditions are the least frequent (18–20%) and unstable conditions are the most common (38–41%); conversely, for 20–80 m interval an isolated WSC maximum is observed in April (0.143), when unstable conditions occur by 27% and the combined neutral and stable conditions by 73%. At the ridge top site of Stone Mt (1300 m, Table 2), monthly α_{30-50} was observed to vary between 0.240 (Nov.) and 0.310 (July) [17]. At the Boulder comparably elevated site of Kingston 14SW (1780 m), monthly α_{10-50} was observed varying 0.113 to 0.137, with maxima in Sep [21]. At the complex terrain site of Albuquerque (2578 m), monthly α_{25-40} ranges between 0.200 (May) and 0.270 (Sep.) [32]. Therefore, similarly to Boulder, at all these elevated locations WSC maxima are reached in summer, and a small WSC intra-annual excursion occurs.

Also turbulence intensity exhibits a narrower variation at monthly than hourly scale, as its overall excursion is 12–18%. Monthly turbulence intensity minima (18.60–22.20%) occur between Feb. and Apr., while turbulence intensity maxima (21.90–25.50%), similarly to WSC, occur in the warmest period. At

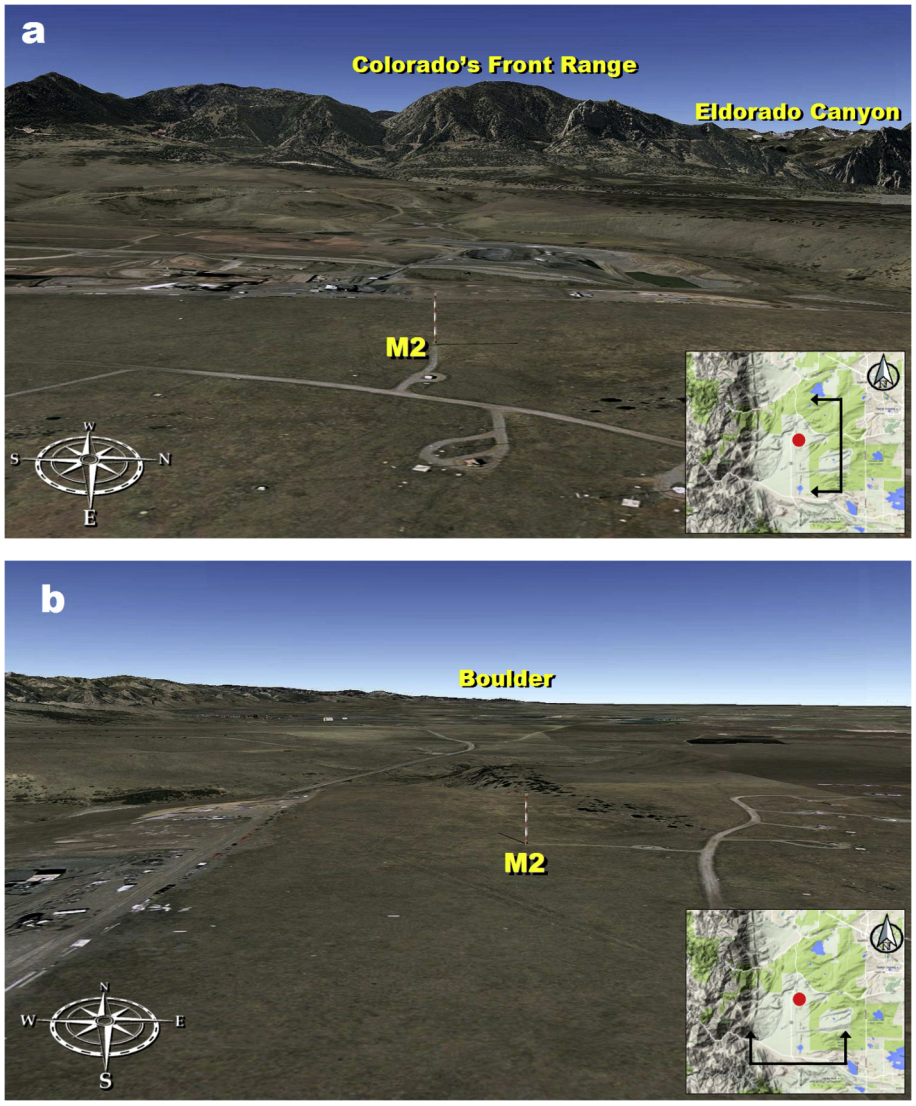

Fig. 2. Aerial view of the M2 met mast as compared to the whole area topography toward West (a) and North (b) directions (Source: GoogleEarth, images of Dec. 2002).

Table 3
Overall annual mean and standard deviation of 10-min records observed between 10 and 80 m at the M2 mast (1997–1998)[a].

Variable	Height AGL (m)							
	10		20		50		80	
	μ	σ	μ	σ	μ	σ	μ	σ
v (m/s)	3.61	2.74	3.96	2.99	4.44	3.41	4.67	3.61
σ_u (m/s)	0.77	0.61	0.79	0.64	0.83	0.67	0.80	0.67
T (°C)	9.38	10.20	9.42	10.18	9.80	10.12	9.66	10.12
ρ (kg/m^3)	1.003	0.035	1.002	0.035	0.997	0.035	0.993	0.035
P (W/m^2)	85.5	282.8	111.3	362.1	159.2	503.1	185.2	570.9

[a] Statistics for the period 01/01/1997–31/12/1998. Valid data: 99.29% (v, T, ρ); 98.95% (σ_u, P).

Table 4
Variation by stability class of 10-min annual turbulence intensity and wind shear coefficient observed between 10 and 80 m at the M2 mast (1997–1998)[a].

	Stability class						
	A	B	C	D	E	F	All
Occurrence (%)	10.49	6.81	11.08	49.25	13.52	8.85	100.00
I_{10} (%)	41.70	30.80	24.90	18.40	17.10	38.00	24.00
I_{20} (%)	40.40	29.40	23.50	17.10	16.00	36.30	22.70
I_{50} (%)	37.90	28.00	22.50	16.40	16.10	33.40	21.50
I_{80} (%)	35.50	26.70	21.50	16.30	15.60	30.70	20.50
α_{10-50}	0.103	0.082	0.087	0.125	0.102	0.183	0.114
α_{10-80}	0.100	0.076	0.078	0.109	0.082	0.193	0.106
α_{20-80}	0.113	0.072	0.070	0.099	0.069	0.226	0.104

[a] Statistics for the period 01/01/1997–31/12/1998. Valid data: 97.21% (stability); 96.43÷97.10% (I), 99.25÷99.76% (α).

the Boulder less elevated site of Stone Mt (Table 2), I_{50} does not exhibit a seasonal course, remarkably only varying 13–14% throughout the year [17]. At the comparably elevated site of Kingston 14SW, observed monthly I_{50} ranges 11% (Jan.) to 16.5% (July) [21]. At the more elevated site of Albuquerque, monthly I_{40} ranges between 9 and 14% [32].

5. Extrapolating wind resource to the WT hub height: results and discussion

5.1. Method's training

During the analysis period (1997–1998), a linear (with no

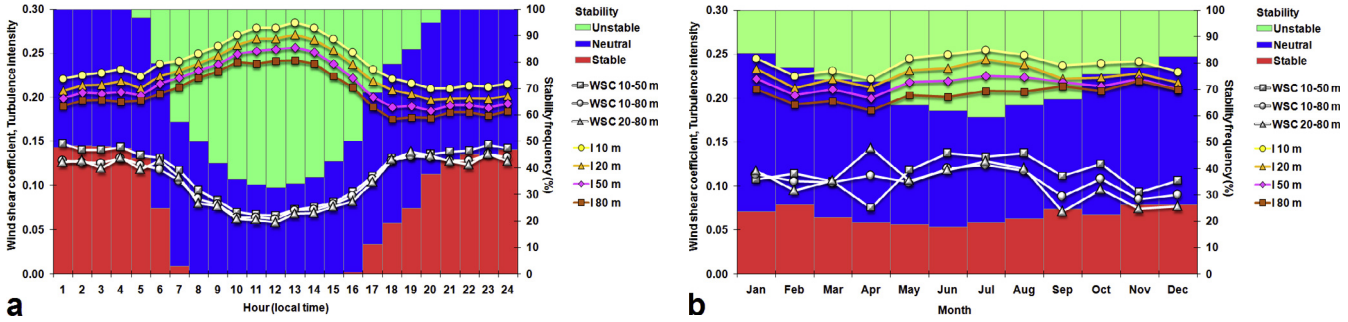

Fig. 3. Variation of 10-min annual mean WSC and turbulence intensity between 10 and 80 m, and occurrence frequency of stability conditions observed at the M2 mast (1997–1998) by: (a) hour of day; (b) month of year.

intercept) regression analysis, sorted by stability class, was applied to Eq. (3). Therefore, the b_{10-50}, b_{10-80}, and b_{20-80} coefficients were obtained by using the following 10-min readings: (i) I_{10} vs. α_{10-50}; (ii) I_{10} vs. α_{10-80}; (iii) I_{20} vs. α_{20-80}.

At Boulder, overall b values range between 1.54 and 1.95: these are the highest b values among all those observed where the method was applied, since they ranged 0.84–0.97 between 10 and 80 m at Cabauw [7], and 1.37–1.45 between 30 and 80 m at FINO3 [8]. Between 10 and 50 m, variation by stability class of b coefficients decreases from class A to a minimum for class E, then increasing for class F, thus exhibiting the same pattern observed at the other two application sites. Across the 10–80 and 20–80 m ranges, a local maximum observed for class B slightly alters this general trend. Therefore, to some extent the hypothesis that the stability-varying b coefficients follow a general rule regardless of the environment under application is confirmed.

5.2. Method's testing: wind resource extrapolation

During the testing period (year 1999), the previously calculated b coefficients (Table 5) were introduced to Eq. (3). Thus, 10-min observed I_{10} and I_{20} records, sorted by stability class, have been used to calculate α_{10-50}, α_{10-80} and α_{20-80}, which then have been used to extrapolate the 10-min observed v_{10} and v_{20} records to 50 and 80 m. Therefore, three extrapolated wind speed values were predicted: (i) v_{50} based on I_{10} observations; (ii) v_{80} based on I_{10} observations; (iii) v_{80} based on I_{20} observations. The statistical results of this analysis are summarized in Table 6.

Overall, in extrapolations to 50 and 80 m annual wind speed observations are over-predicted by 1–5%, with NRMSE ranging 0.17–0.23, IA 0.98–0.99, and r 0.96–0.98.

In the 10–50 m wind speed extrapolation, overall scores obtained at Boulder are a bit finer than those achieved in the 10–40 m extrapolation at Cabauw by applying the same method (NB = 4%, NRMSE = 0.16, IA = 0.98, r = 0.95 [7]). In the 10–80 m and 20–80 m extrapolations, Boulder scores are similar to those achieved in the 10–50 m extrapolation, yet with a slightly worse NB. Again compared, according to the same height intervals, to the results obtained at Cabauw by using the same method, these 80-m Boulder scores are slightly better: in the 10–80 m extrapolation, this is evidenced by NB = 4% (vs. 6%), NRMSE = 0.23 (vs. 0.24), IA = 0.98 (vs. 0.92), and r = 0.96 (vs. 0.86); in the 20–80 m extrapolation, this is evidenced by NB = 5% (vs. 7%), NRMSE = 0.19 (vs. 0.20), IA = 0.99 (vs. 0.94), and r = 0.98 (vs. 0.91). If comparing the 20–80 m wind speed extrapolation at Boulder to the 30–80 m one at FINO3, scores are generally similar, as exhibiting the same NB (5%), NRMSE = 0.19 (vs. 0.20), IA = 0.99 (vs. 0.96), and r = 0.98 (vs. 0.94).

Method's overall accuracy in the 10–50 m wind speed extrapolation at Boulder (NB = 1%) is similar to the one (NB = 1.5%) achieved at the same M2 mast between 20 and 50 m by Lubitz [5], who applied the PL using the α calculated between 10 and 20 m (via Eq. (1)). Current 10–50 m method's performances at Boulder are

Table 5
Variation by stability class of b coefficients of α–I linear relationship (Eq. (3)) resulting from 10-min observations between 10 and 80 m at the M2 mast (1997–1998)[a,b].

	Stability class						
	A	B	C	D	E	F	All
b_{10-50}	4.14	4.03	3.18	1.42	0.96	1.65	1.95
b_{10-80}	3.65	3.93	2.98	1.42	0.97	1.49	1.86
b_{20-80}	2.68	3.21	2.56	1.26	0.73	1.12	1.54

[a] Statistics for the period 01/01/1997–31/12/1998. Valid data: 97.21%.
[b] b_{12} denotes b coefficients calculated from α_{12} and I_1 observations.

Table 6
Statistical values by stability conditions of 10-min wind speed at 50 and 80 m observed and predicted by the I vs. α linear relationship (Eq. (3)) at the M2 mast during the testing period (1999)[a].

Height AGL (m)		Stability conditions			
		Unstable	Neutral	Stable	All
50	Observed				
	N (%)	13436 (27.26)	25085 (50.90)	10765 (21.84)	49286 (100)
	μ_O (m/s)	3.06	6.74	2.78	4.87
	σ_O (m/s)	1.50	4.63	1.39	3.95
	Predicted using observed I_{10}				
	μ_P (m/s)	2.97	6.78	2.95	4.91
	σ_P (m/s)	1.43	4.82	1.31	4.05
	NB	0.03	−0.01	−0.06	−0.01
	NRMSE	0.16	0.14	0.34	0.17
	IA	0.97	0.99	0.86	0.99
	r	0.95	0.98	0.75	0.98
80	Observed				
	N (%)	13436 (27.26)	25085 (50.90)	10765 (21.84)	49286 (100)
	μ_O (m/s)	3.13	7.04	2.92	5.07
	σ_O (m/s)	1.65	4.92	1.60	4.20
	Predicted using observed I_{10}				
	μ_P (m/s)	3.14	7.26	3.32	5.27
	σ_P (m/s)	1.49	5.19	1.49	4.35
	NB	0.00	−0.03	−0.13	−0.04
	NRMSE	0.22	0.18	0.45	0.23
	IA	0.95	0.98	0.77	0.98
	r	0.91	0.97	0.62	0.96
	Predicted using observed I_{20}				
	μ_P (m/s)	3.20	7.28	3.34	5.31
	σ_P (m/s)	1.52	5.14	1.52	4.32
	NB	−0.02	−0.03	−0.13	−0.05
	NRMSE	0.19	0.14	0.39	0.19
	IA	0.96	0.99	0.84	0.99
	r	0.94	0.98	0.74	0.98

[a] Statistics for the period 01/01/1999–31/12/1999. Sample size: 93.77%.

slightly better than those obtained in the 20–40 m wind speed extrapolation by Bañuelos-Ruedas et al. [30] at the rural site of UAA-UAZ (2230 m, Table 2): in predicting actual v_{40}, by applying the LogL they found an NB of 2.5%, while using the PL with α calculated between 20 and 40 m they found an NB of 5.7%. If analysed in the 10–80 m wind speed extrapolation at Boulder, current method agrees with the PL applied by Lubitz [5] across the same height interval based on the same M2 mast data by using the 1/7 α value, as NB = 4% is returned (vs. 4.4% by Lubitz [5]). Focussing on the Boulder 20–80 m extrapolation and again comparing current scores (NB = 5%) with those achieved through the PL by Lubitz [5], the α–I method is conversely outperformed, as he found NB = 0.6% using the $\alpha_{10\text{-}20}$ value, and NB = 2.7% using the 1/7 α value. On the contrary, current 20–80 m method's results at Boulder conform to those achieved by Lackner et al. [28] across the same height range based on the same M2 mast data: in predicting actual v_{80}, by applying the LogL they found an NB of 5%, while using the PL with α calculated between 20 and 50 m they found an NB of 6%. At the same site, a slightly finer score (NB = 3.3%) to predict the observed v_{80} was achieved by Elkinton et al. [27] by using the LogL.

Summarising, comparison of the α–I method's scores achieved at Boulder in 50-m and 80-m wind speed extrapolations to those reported in the literature leads to conclude that its accuracy substantially agrees with the one achieved by either LogL or PL. However, in all the above-cited works both PL and LogL were applied over the same sample (intra-sample testing) used to calculate their respective surface parameters (i.e. z_0 and α), whereas the α–I method was tested over a period following the training one, i.e. when its surface parameters (the b coefficients) were calculated: therefore, unlike the former laws, current method was actually applied as a pure predicting model.

The analysis by atmospheric stability conditions highlights the crucial role played by this parameter on method's skills. Similar performances are returned for both unstable and neutral conditions. In particular, time variation of the observed upper winds is best fitted when wind speed extrapolation involves the strongest neutral winds, as indicated by the highest r values achieved (0.97–0.98). Conversely, scores are worse under stable conditions, particularly in the 10–80 m extrapolation (NRMSE = 0.45, IA = 0.77, r = 0.62). The same outcome was found at the other two method's application sites, thus confirming serious concerns about method's applicability under stable conditions. However, at Boulder method's performances for stable conditions are finer than those achieved at the other two sites, as shown by all statistical indicators: markedly, current NB is 6–13%, while it was 12–14% at Cabauw [7], and 28–32% at FINO3 [8].

Method's wind resource extrapolating capability has been also assessed through the annual Weibull probability density function between observed and predicted wind speed records (Fig. 4).

As shown in Table 2, at Boulder the k parameter observed at 50 m (1.72, Fig. 4a) is comparable to the values of 1.70 achieved at 50 m at Tonopah 24NW (1535 m) [21], 1.73 observed at 45.7 m at Livingston (1420 m) [22], and 1.78 measured at 45.7 m at Boone (1347 m) [20]. This Boulder k_{50} value is higher than the 1.33–1.41 range observed at 50 m at three ridge locations in US with elevation ranging 1354–1780 m [21], and than the 1.60 value achieved at 40 m at the similarly elevated, semi-desert site of Shahrbabak [25]. Conversely, it is lower than the 1.96 value achieved at 40 m at the desert site of Rafsanjan (1550 m) [25], and than the 1.92–2.00 range observed at 45.7 m at three locations in US with elevation ranging 1859–2290 m [22]. This Boulder k_{50} value is also lower than the values of 2.24 observed at 45.7 m at the open grassland site of Clayton (1536 m) [20], 2.60 at 50 m at the ridgetop site of Stone Mt (1300 m) [17], and 2.63 at 45.7 m at the barren, flat hilltop site of Tucumcari (1354 m) [22]. On the other hand, the k parameter measured at 80 m at Boulder (1.60, Fig. 4b) is lower than the value of 1.79 measured at 76.2 m at the forested ridgetop rough site of Boone (1347 m) [20]. This survey on various mountain locations worldwide thus brings to the conclusion that the k values exhibit a quite wide range, and that a reference k value, specific of mountain sites, cannot be clearly ascertained.

At 50 m (Fig. 4a), observed wind speed Weibull distribution at Boulder is finely reproduced by the predicted curve, not only by scale (c over-predicted by 0.8%), but also by shape (k over-predicted by 2.9%), with median wind speed (3.65 m/s) biased by 4.1%. Scores achieved at 80 m (Fig. 4b) returns over-predictions of 4.4–5.2% for c and 11.9–12.5% for k, with median wind speed (3.79 m/s) biased by ±1.1%. Although the v_{10-80} and v_{20-80} predicted curves almost match, in predicting the observed v_{80} distribution the use of I_{10} rather than I_{20} observations is preferable as the actual median wind speed is slightly under- rather than over-predicted.

Method's wind speed Weibull distribution fitting at Boulder proved to be finer than the one achieved at Cabauw, where between 10 and 50 m median wind speed was biased by 7% and k by 20%, while in the 10–80 m and 20–80 m extrapolations median wind speed values were biased by 10.3–11.4% and k by 20–27% [7]. Conversely, method's skills at Boulder between 20 and 80 m are comparable to those exhibited between 30 and 80 m at FINO3, markedly as concerns median wind speed, which was biased by 1.4% (vs. 1.1% at Boulder) [8].

5.3. Method's testing: wind energy yield estimation

To assess method's capability in calculating the annual energy yield, two groups of commercial WTs have been selected, with hub height approximately equal to 50 and 80 m, respectively, and different rated power [43–47]. Their power curves are plotted in Fig. 4.

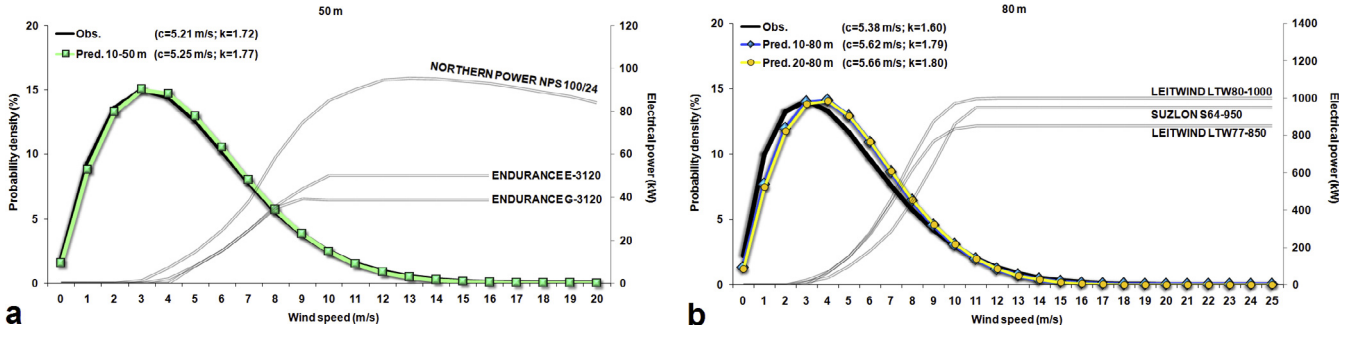

Fig. 4. Annual wind speed Weibull distribution observed and predicted at the M2 mast during the testing period (1999): (a) 50 m using I_{10}; (b) 80 m using I_{10} and I_{20}. The power curves of WTs used in wind energy yield calculation are also shown.

Table 7
Annual wind energy yield parameters calculated at 50 m at the M2 mast using a single WT and relative difference of predictions compared to observations (1999)[a,b,c]. WTs used: 35-kW Endurance G-3120 [43], 50-kW Endurance E-3120 [44], and 95-kW Northern Power NPS 100/24 [45].

WT (Rated power)		50-m converted energy				
		AF (%)	*CF* (%)	*FLH* (h/y)	*AEY* (MWh/y)	Total losses (%)
Endurance G-3120 (35 kW)	Observed					
	μ_O	56.37	22.23	1949	68.2	12.15
	Predicted using I_{10}					
	μ_P	57.39	22.42	1965	68.8	
	NE (%)	−1.82	−0.85			
Endurance E-3120 (50 kW)	Observed					
	μ_O	56.37	17.34	1521	76.0	12.15
	Predicted using I_{10}					
	μ_P	57.39	17.44	1530	76.5	
	NE (%)	−1.82	−0.57			
Northern Power NPS 100/24 (95 kW)	Observed					
	μ_O	63.37	15.73	1379	131.0	13.59
	Predicted using I_{10}					
	μ_P	64.45	15.80	1385	131.6	
	NE (%)	−1.70	−0.44			

[a] Statistics for the period 01/01/1999–31/12/1999. Sample size: 93.77%.
[b] Air density normalisation to actual value applied based on 10-min observed air density values to account for deviations from the standard value (1.225 kg/m^3), according to prescriptions of [40].
[c] Total losses accounted for observed and predicted energy yield are a combination of WT- and site-specific losses: their single values are reported in Ref. [48].

Since Boulder is a high altitude site, thus affected by air density values significantly lower (Table 3) than the reference value (1.225 kg/m^3) of WT power curves provided by manufacturers, the air density normalisation procedure recommended in Ref. [40] has been applied based on air density values observed each 10 min during the testing period. Overall energy losses have been calculated as a combination of: (i) WT-specific losses (for gearbox, generator, converter, and unavailability & repair); (ii) site-specific losses (for electric grid connection and icing). Full details of this approach may be found in Ref. [48]. Since computations are referred to single WTs and not a whole wind farm, losses due to WT wakes (array losses) were not considered.

As expected since a "class 1" location (see Section 4), from observations at 50 m (Table 7) not a remarkable wind energy output can be extracted from the Boulder site, as shown by the 15.73–22.23% range achieved for *CF* (corresponding to *FLH* = 1379–1949 h/y): this means that a wind farm project in the area is not economically viable. Aside from the low mean air density values (Table 3), this outcome was also expected due to the relevant occurrence of stable conditions (21.84%, Table 6), and thus remarkable power deficits [3].

In terms of method's skill, the *CF*-related NE returns a 0.44–0.85% range, which was expected following the finely reproduced observed v_{40} Weibull distribution (Fig. 4a), particularly for the higher wind speed regimes relevant for WTs. Current 10–50 m performances at Boulder are better than the corresponding 10–40 m ones achieved at Cabauw, where the *CF* values were biased by 5.54–5.80% [7]. These 10–50 m Boulder scores are comparable to those obtained by Đurišić and Mikulović [19] in the 10–60 m extrapolation over the mountain site with moderately complex terrain of Duga Poljane, Serbia (1310 m ASL, Table 2): by using the PL with the annual average α value (0.190), by employing a 500-kW WT they achieved a 1.25% bias in estimating *AEY*.

At Boulder, wind energy potential is even lower if an 80-m hub height WT is supposed to be installed (Table 8): the most efficient solution returns a *CF* value of 20.39%.

Method's performances in predicting energy yield at 80 m are worse than those of 10–50 m extrapolation: the 10–80 m extrapolation returns *CF* values biased by 2.79–5.00%, while the 20–80 m extrapolation *CF* values biased by 4.38–6.44%. Both extrapolations to 80 m provide a certain *AEY* over-estimation, which was expected if considering their slightly optimistic tendency to predict the observed Weibull distribution wind regimes most fruitful for WTs (Fig. 4b). However, both in 10–80 m and 20–80 m extrapolations method's accuracy at Boulder is again higher than the one observed across the same height intervals at Cabauw, where *CF* values were biased by more than a double amount: 10.20–10.73% in the 10–80 m extrapolation, and 14.25–14.47% in the 20–80 m extrapolation [7]. This outcome is noteworthy if considering Cabauw is a flat and homogeneous site, whereas Boulder is a mountain and fairly complex terrain site. Conversely, current Boulder scores between 20 and 80 m are worse than those achieved between 30 and 80 m at the FINO3 offshore site, where application of the same method returned *CF* values biased by 0.41–1.02% [8]. At Boulder, method's accuracy in predicting *AEY* across the 20–80 m extrapolation (bias of 4.38–6.44%) is lower than the corresponding one achieved by Lubitz [5] through the PL at the same site and across the same interval: by employing a 1650-kW WT, he achieved a 0.6% bias using the 1/7 α value, and basically an unbiased estimation using the $\alpha_{10\text{-}20}$ overall value. However, within both these works by Lubitz [5], and Đurišić and Mikulović [19], which represent two of the few wind resource extrapolating applications over mountain locations, the PL was again intra-sampling tested.

6. Conclusions

The α–*I* wind resource extrapolating method has been tested over the NWTC elevated (1855 m) mountain site near Boulder, affected by a complex terrain. The following conclusions may be drawn on method's application to predict 50-m and 80-m wind speed values:

- overall values of linear regression coefficients *b* exhibit the highest and widest range (1.54–1.95) compared to those observed at the flat onshore (0.84–0.97) and offshore (1.37–1.45) site;
- aside from a local exception across the 10–80 and 20–80 m ranges, variation by stability class of *b* coefficients follows the same rule observed at both Cabauw and FINO3: this confirms that, to some extent, their stability variability is environment-independent;

Table 8
Annual wind energy yield parameters calculated at 80 m at the M2 mast using a single WT and relative difference of predictions compared to observations (1999)[a,b,c]. WTs used: 850-kW Leitwind LTW77-850 [46], 950-kW Suzlon S64-950 [47], and 1000-kW Leitwind LTW80-1000 [46].

WT (Rated power)		80-m converted energy				
		AF (%)	*CF* (%)	*FLH* (h/y)	*AEY* (MWh/y)	Total losses (%)
Leitwind LTW77-850 (850 kW)	Observed					
	μ_O	63.14	20.39	1787	1519.6	13.59
	Predicted using I_{10}					
	μ_P	67.92	21.41	1876	1595.4	
	NE (%)	−7.57	−5.00			
	Predicted using I_{20}					
	μ_P	68.39	21.70	1903	1617.4	
	NE (%)	−8.31	−6.44			
Suzlon S64-950 (950 kW)	Observed					
	μ_O	64.21	15.00	1316	1249.6	13.59
	Predicted using I_{10}					
	μ_P	69.07	15.42	1352	1284.4	
	NE (%)	−7.57	−2.79			
	Predicted using I_{20}					
	μ_P	69.55	15.66	1373	1303.7	
	NE (%)	−8.31	−4.38			
Leitwind LTW80-1000 (1000 kW)	Observed					
	μ_O	63.14	18.71	1639	1639.8	11.93
	Predicted using I_{10}					
	μ_P	67.92	19.57	1716	1715.4	
	NE (%)	−7.57	−4.61			
	Predicted using I_{20}					
	μ_P	68.39	19.85	1740	1740.3	
	NE (%)	−8.31	−6.13			

[a] Statistics for the period 01/01/1999–31/12/1999. Sample size: 93.77%.
[b] Air density normalisation to actual value applied based on 10-min observed air density values to account for deviations from the standard value (1.225 kg/m^3), according to prescriptions of [40].
[c] Total losses accounted for observed and predicted energy yield are a combination of WT- and site-specific losses: their single values are reported in Ref. [48].

- the method is reliable in extrapolating wind speed to 50 and 80 m, with mean values over-predicted by 1–5%, NRMSE = 0.17–0.23, and r = 0.96–0.98;
- in the 10–50 m wind speed extrapolation, scores at Boulder are a bit finer than those achieved in the 10–40 m extrapolation at Cabauw;
- in the 10–80 m and 20–80 m wind speed extrapolations, scores at Boulder are better than those achieved at Cabauw across the same height intervals: NB = 4–5% (vs. 6–7%), NRMSE = 0.19–0.23 (vs. 0.20–0.24), IA = 0.98–0.99 (vs. 0.92–0.94), and r = 0.96–0.98 (vs. 0.86–0.91);
- scores from the 20–80 m wind speed extrapolation at Boulder are similar to those achieved in the 30–80 m extrapolation at FINO3, as exhibiting the same NB (5%), NRMSE = 0.19 (vs. 0.20), IA = 0.99 (vs. 0.96), and r = 0.98 (vs. 0.94);
- the method is confirmed being strongly sensitive to the different stability conditions: finer performances are returned for both unstable and neutral conditions (NRMSE = 0.14–0.22, IA = 0.95–0.99, r = 0.91–0.98), while less accurate for stable conditions (NRMSE = 0.34–0.45, IA = 0.77–0.86, r = 0.62–0.75); however, on a mountain site the method is less stability-sensitive than it was on the flat onshore and particularly on the offshore site;
- at Boulder, method's performances for stable conditions (NB = 6–13%) are slightly and largely finer than those achieved at the other two sites, respectively, as NB was 12–14% at Cabauw, and 28–32% at FINO3; thus, under stable conditions method's application on a mountain site could be performed with more confidence than elsewhere;
- at Boulder, both 50-m and 80-m observed annual Weibull distributions are finely predicted by the corresponding extrapolated distributions (bias of median wind speed within 4.1%); scores are better than at Cabauw, while comparable to those at FINO3;
- current Boulder scores are comparable to those reported in the literature and achieved by applying either LogL or PL.

The method returned *CF* values biased by 0.44–0.85% (10–50 m), 2.79–5.00% (10–80 m), and 4.38–6.44% (20–80 m extrapolation). These scores are finer than those obtained at comparable height ranges at Cabauw, where *CF* values were biased by 5.54–5.80% (10–40 m), 10.20–10.73% (10–80 m), and 14.25–14.47% (20–80 m extrapolation). Conversely, Boulder scores between 20 and 80 m are worse than those between 30 and 80 m at FINO3, where *CF* was biased by 0.41–1.02%.

Applications of wind resource extrapolating methods to predict *AEY* over mountain sites are numbered in the literature to address a thorough comparison. With respect to outcomes from two of the few, current method proved to be: (i) in the 10–50 m extrapolation, comparable to the PL applied in the 10–60 m extrapolation in Serbia (1310 m) using the annual α value, which returned a bias of 1.25%; (ii) in the 20–80 m extrapolation, outperformed by the PL applied at the same site and across the same interval, which basically returned an unbiased estimation. However, since tested over the same sample used for calculating the α values, in both those cases the PL was not applied as a pure predicting model such as α–I, which conversely was tested over a period independent on the one used for training. In any case, practical usefulness of this method for wind energy studies is confirmed: (i) by solely using 10-min records of wind speed (mean and standard deviation) routinely collected at surface heights, the method is confident to predict energy yield at WT hub height; (ii) since calculating a 10-min dynamically-varying α value, the method enables the PL to suitably adjust its shape to the various roughness and stability conditions affecting the site each time frame; (iii) method's scores improve under the most energetic conditions (i.e. when the strongest neutral winds occur), and thus when its accuracy is more urgent.

Summarising, the method proved its reliability also when applied at a site: (i) located on elevated mountain and affected by fairly complex terrain, which is of particular relevance if bearing in mind the PL the method is based upon was actually developed for flat and homogeneous terrain; (ii) not exhibiting a relevant wind energy potential (*CF* at best of 22.23%), thus where – according to the previous onshore and offshore applications – a lower method's accuracy was expected; (iii) where the occurrence of stable conditions is significant (21.84%), thus when – according to the previous applications – a lower method's accuracy was expected.

Acknowledgements

The M2 mast data used in this work have been downloaded from the National Wind Technology Center (NWTC, http://www.nrel.gov/midc/nwtc_m2), managed by the National Renewable Energy Laboratory (NREL) for the US Department of Energy.

References

[1] M.S. Adaramola, M. Agelin-Chaab, S.S. Paul, Assessment of wind power generation along the coast of Ghana, Energ Convers. Manage 77 (2014) 61–69.
[2] M.C. Holtslag, W.A.A.M. Bierbooms, G.J.W. van Bussel, Extending the diabatic surface layer wind shear profile for offshore wind energy, Renew. Energy 101 (2017) 96–110.
[3] D.A. Spera, Wind Turbine Technology: Fundamental Concepts of Wind Turbine Engineering, second ed., ASME Press, New York, 2009.
[4] B.L. Sill, Turbulent boundary layer profiles over uniform rough surfaces, J. Wind Eng. Ind. Aerodyn. 31 (2) (1988) 147–163.
[5] W.D. Lubitz, Power law extrapolation of wind measurements for predicting wind energy production, Wind Eng. 33 (3) (2009) 259–271.
[6] G. Gualtieri, Atmospheric stability varying wind shear coefficients to improve wind resource extrapolation: a temporal analysis, Renew. Energy 87 (2016) 376–390.
[7] G. Gualtieri, Surface turbulence intensity as a predictor of extrapolated wind resource to the turbine hub height, Renew. Energy 78 (2015) 68–81.
[8] G. Gualtieri, Surface turbulence intensity as a predictor of extrapolated wind resource to the turbine hub height: method's test at an offshore site, Renew. Energy 111 (2017) 175–186.
[9] C.D. Whiteman, Mountain Meteorology: Fundamentals and Applications, Oxford University Press, Oxford and New York, 2000.
[10] T. Burton, D. Scarpe, N. Jenkins, E. Bossanyi, Wind Energy Handbook, John Wiley & Sons, Chichester, UK, 2001.
[11] J.F. Manwell, J.G. McGowan, A.L. Rogers, Wind Energy Explained: Theory, Design and Application, second ed., John Wiley & Sons, Chippenham,UK, 2010.
[12] M. Burlando, A. Podestà, L. Villa, C.F. Ratto, G. Cassulo, Preliminary estimate of the large-scale wind energy resource with few measurements available: the case of Montenegro, J. Wind Eng. Ind. Aerodyn. 97 (11) (2009) 497–511.
[13] D. Carvalho, A. Rocha, C.S. Santos, R. Pereira, Wind resource modelling in complex terrain using different mesoscale-microscale coupling techniques, Appl. Energy 108 (2013) 493–504.
[14] D. Hanslian, J. Hošek, Combining the VAS 3D interpolation method and Wind Atlas methodology to produce a high-resolution wind resource map for the Czech Republic, Renew. Energy 77 (2015) 291–299.
[15] M. Gonçalves-Ageitos, A. Barrera-Escoda, J.M. Baldasano, J. Cunillera, Modelling wind resources in climate change scenarios in complex terrains, Renew. Energy 76 (2015) 670–678.
[16] A. González, J.C. Pérez, J.P. Díaz, F.J. Expósito, Future projections of wind resource in a mountainous archipelago, Canary Islands, Renew. Energy 104 (2017) 120–128.
[17] B.W. Raichle, W.R. Carson, Wind resource assessment of the southern Appalachian Ridges in the southeastern United States, Renew. Sust. Energ Rev. 13 (5) (2009) 1104–1110.
[18] A. Ucar, F. Balo, Evaluation of wind energy potential and electricity generation at six locations in Turkey, Appl. Energy 86 (10) (2009) 1864–1872.
[19] Ž. Đurišić, J. Mikulović, A model for vertical wind speed data extrapolation for improving wind resource assessment using WAsP, Renew. Energy 41 (2012) 407–411.
[20] W.F. Sandusky, D.S. Renné, Candidate Wind Turbine Generator site annual data. Summary for January 1979 through December 1979. PNL-3703, Pacific Northwest Lab., Richland, WA, USA, March 1981.
[21] R. Belu, D. Koracin, Wind characteristics and wind energy potential in western Nevada, Renew. Energy 34 (10) (2009) 2246–2251.
[22] W.F. Sandusky, J.W. Buck, D.S. Renné, D.L. Hadley, O.B. Abbey, S.L. Bradymire, et al., Candidate Wind Turbine Generator Site Cumulative Meteorological data. Summary and data for January 1982 through September 1982. PNL-4663, Pacific Northwest Lab., Richland, WA, USA, Aug. 1983.
[23] A. Ouammi, R. Sacile, A. Mimet, Wind energy potential in Liguria region, Renew. Sust. Energ Rev. 14 (1) (2010) 289–300.
[24] F. González-Longatt, H. Medina, J.S. González, Spatial interpolation and orographic correction to estimate wind energy resource in Venezuela, Renew. Sust. Energ Rev. 48 (2015) 1–16.
[25] O. Alavi, A. Sedaghat, A. Mostafaeipour, Sensitivity analysis of different wind speed distribution models with actual and truncated wind data: a case study for Kerman, Iran. Energ Convers. Manage 120 (2016) 51–61.
[26] M. Mpholo, T. Mathaba, M. Letuma, Wind profile assessment at Masitise and Sani in Lesotho for potential off-grid electricity generation, Energ Convers. Manage 53 (1) (2012) 118–127.
[27] M.R. Elkinton, A.L. Rogers, J.G. McGowan, An investigation of wind-shear models and experimental data trends for different terrains, Wind Eng. 30 (4) (2006) 341–350.
[28] M.A. Lackner, A.L. Rogers, J.F. Manwell, J.G. McGowan, A new method for improved hub height mean wind speed estimates using short-term hub height data, Renew. Energy 35 (10) (2010) 2340–2347.
[29] K. Smith, G. Randall, D. Malcolm, N. Kelley, B. Smith, Evaluation of Wind Shear Patterns at Midwest Wind Energy Facilities, in: NREL/CP-500–32492, Wind-Power Conference, National Renewable Energy Laboratory, Portland, OR, USA, 2002.
[30] F. Bañuelos-Ruedas, C. Angeles-Camacho, S. Rios-Marcuello, Analysis and validation of the methodology used in the extrapolation of wind speed data at different heights, Renew. Sust. Energ Rev. 14 (8) (2010) 2383–2391.
[31] Y. Cancino-Solórzano, J. Xiberta-Bernat, Statistical analysis of wind power in the region of Veracruz (Mexico), Renew. Energy 34 (6) (2009) 1628–1634.
[32] Sandia National Laboratories, New Mexico Wind Resource Assessment: lee Ranch, Global Energy Concepts, LLC, U. S. A., Feb. 2003.
[33] J. Counihan, Adiabatic atmospheric boundary layers: a review and analysis of data collected from the period 1880–1972, Atmos. Environ. 9 (1975) 871–905.
[34] H. Ishizaki, Wind profiles, turbulence intensities and gust factors for design in Typhoon-prone regions, J. Wind Eng. Ind. Aerodyn. 13 (1983) 55–66.
[35] D. Jager, A. Andreas, NREL National Wind Technology Center (NWTC): M2 Tower; Boulder, Colorado (Data). NREL Report No. DA-5500–56489, Sep. 1996, https://doi.org/10.5439/1052222.
[36] A. Clifton, S. Schreck, G. Scott, N. Kelley, J.K. Lundquist, Turbine inflow characterization at the national wind technology center, J. Sol. Energy Eng. 135 (3) (2013) 031017.
[37] A. Clifton, J.K. Lundquist, Data clustering reveals climate impacts on local wind phenomena, J. Appl. Meteorol. 51 (8) (2012) 1547–1557.
[38] R.M. Banta, L.D. Olivier, P.H. Gudiksen, Sampling requirements for drainage flows that transport atmospheric contaminants in complex terrain, Radiat. Prot. Dosim. 50 (2–4) (1993) 243–248.
[39] R. Sozzi, T. Georgiadis, M. Valentini, Introduzione Alla Turbolenza Atmosferica, Bologna, Italy: Pitagora, 2002 [in Italian].
[40] International Electrotechnical Commission (IEC), IEC 61400-12-1. Wind Turbines–part12-1: Power Performance Measurements, first ed., 2005. Geneva, Switzerland.
[41] Environmental Protection Agency (EPA), Meteorological Monitoring Guidance for Regulatory Modeling Applications. EPA-454/R-99–9005, Research Triangle Park, NC, USA, Feb. 2000.
[42] J.S. Touma, Dependence of the wind profile power law on stability for various locations, J. Air Pollut. Control Assoc. 27 (9) (1977) 863–866.
[43] Dailye. Endurance G-3120 technical specifications; Available: http://www.dailyenmoveme.com/sites/dailyenmoveme.com/files/G-3120-Product-Brochure_35.pdf (Accessed 14 November 2017).
[44] Maden Eco Ltd. Endurance E-3120 technical specifications; Available at: http://www.madeneco.co.uk/wind-turbines/products (Accessed 14 November 2017).
[45] Northern Power Systems. NPS 100/24 technical specifications; Available at: http://www.northernpower.com (Accessed 14 November 2017).
[46] Leitwind wind turbines. LTW77–850 and LTW80-1000 technical specifications; Available at: http://en.leitwind.com (Accessed 14 November 2017).
[47] WindPower, The wind turbines and wind farms database, 2017. http://www.thewindpower.net (Accessed 14 November 2017).
[48] G. Gualtieri, Improving investigation of wind turbine optimal site matching through the self-organizing maps, Energ Convers. Manage 143 (2017) 295–311.